Investigating the $N = 28$ shell-closure with single-nucleon transfer reactions

Aditya Babu[1,*], *A. J.* Mitchell[1,**], *Benjamin. P* Kay[2], *Yassid* Ayyad[3], *Khushi* Bhatt[2,4], *B. Alex* Brown[5], *Frank* Browne[6], *Zoe* Crowley-Burrows[1], *Benjamin J.* Coombes[1], *Sean J.* Freeman[6], *Abhijith A.* Gopakumar[1], *Calem R.* Hoffman[2], *Luke E.* Johnstone[1], *Vasil* Karayonchev[2], *Anna* Kawecka[7], *Thomas* Kitchen[1], *Gregory J.* Lane[2], *Juan* Lois-Fuentes[5], *Eilens* Lopez-Saveedra[2], *Thomas* Perissinotto[1], *Andrew E.* Stuchbery[1], *T. L* Tang[2], *Daniel* Tempra[1], *Ivan A.* Tolstukhin[2], *Nate* Watwood[2], *Jack A.* Woodside[1], and *Alan H.* Wuosmaa[8]

[1]Department of Nuclear Physics and Accelerator Applications, The Australian National University, Canberra, ACT 2601, Australia
[2]Physics Division, Argonne National Laboratory, Lemont, IL 60439, USA
[3]IGFAE, Universidade de Santiago de Compostela, E-15782, Santiago de Compostela, Spain
[4]Department of Physics and Astronomy, University of Notre Dame, Notre Dame, 46556, IN, USA
[5]Facility for Rare Isotope Beams, Michigan State University, East Lansing, MI, USA
[6]Department of Physics and Astronomy, University of Manchester, Manchester, M13 9PL, United Kingdom
[7]Department of Physics, Chalmers University of Technology, Chalmersgatan 4, 412 96 Gothenburg, Sweden
[8]Department of Physics, University of Connecticut, Storrs, 06269, CT, USA

Abstract. We report on a first-of-its-kind simultaneous ^{48}Ca(d, p) and ^{48}Ca(d, t) reactions study in inverse kinematics with the Helical Orbit Solenoidal Spectrometer (HELIOS) at Argonne National Laboratory. This serves as an important demonstration of the viability of simultaneous reaction studies with solenoidal spectrometers, paving the way for similar experiments at other facilities, including with the SOLARIS device at FRIB. Furthermore, we report on the development of the new Light-Ion Focal Plane Detector (L-ion FPD) to perform complementary single-nucleon transfer reactions with light beams and enriched, stable targets with the Enge Magnetic Spectrometer at the Heavy Ion Accelerator Facility (HIAF).

1 Introduction

The calcium ($Z = 20$) nuclides have long been considered "textbook" shell-model nuclei, with known doubly magic isotopes at $N = 20, 28$ and new, proposed shell gaps emerging at $N = 32, 34$. However, a growing body of evidence suggests that further investigation of the shell model is required in this region to explain the emergent shell closures [1].

In ^{48}Ca, an unexpected reduction of the $\nu f_{7/2}$ strength was observed from neutron-knockout reactions from the $f_{7/2}$ ground states of ^{48,50}Ca [2]. This is inconsistent with shell-model predictions using both phenomenological effective-interaction Hamiltonians like GXPF1 and microscopically derived $NN + 3N$ interactions in the pf model space. Furthermore, this result is also in disagreement with spectroscopic strengths determined from single-nucleon transfer reactions, although the historical data here are sparse [3, 4].

The nuclide ^{48}Ca is also a candidate for neutrinoless double-beta decay and precise knowledge of ground-state properties in the decay candidate and its corresponding decay product, ^{48}Ti, including the occupancies of the neutron and proton fp-shell orbitals, are important to constrain calculations of the decay matrix element [5]. Additionally, the emergent shell closures at $N = 32, 34$ prompt a further need for systematic studies of effective single-particle energies across the region, as summarised in Fig. 1 [6–9]. With new facilities like the Facility for Rare Isotope Beams (FRIB) coming online, there is now greater scope to advance investigations of exotic nuclides beyond $N = 28$ with single-nucleon transfer reactions and particle-spectroscopy techniques. Complementary investigations of stable isotopes along the $N = 28$ chain are also needed to benchmark results and establish a clear picture of the evolution of nuclear structure in the region.

2 Simultaneous reaction studies with solenoidal spectrometers

Solenoidal spectrometers are an excellent tool to perform transfer-reaction studies with heavy beams and light targets in the inverse kinematics regime. The principles of operation of such devices is described in Ref. [10]. The Helical Orbit Spectrometer (HELIOS) [11] was the first solenoidal spectrometer of this kind to be developed for such studies. It is located at the ATLAS facility at Argonne National Laboratory (ANL). Today, it is one of three such instruments in the world, along with the SOLARIS spectrometer at FRIB [12, 13] and the ISOLDE Solenoidal Spectrometer (ISS) at HIE-ISOLDE [14]. All three devices can further be operated as Active Target Time Projection Chambers.

*e-mail: aditya.babu@anu.edu.au
**e-mail: aj.mitchell@anu.edu.au

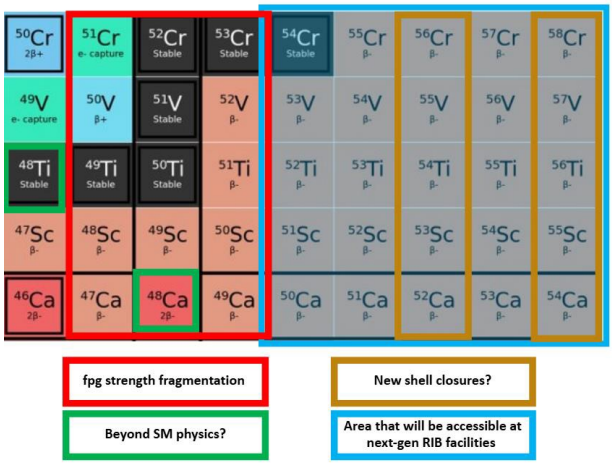

Figure 1. The region around doubly magic ^{48}Ca with isotopes of interest highlighted.

All three devices operate on the same principles. The heavy-ion beam enters a large-bore solenoid and passes through hollow, tubular position-sensitive silicon detectors aligned along the solenoid axis. The beam then impinges on a light target, positioned normal to the solenoid axis. The targets sit on an adjustable fan which can accommodate up to eight targets. The various light reaction products subsequently undergo cyclotron motion under the Lorentz force and are intercepted by the Si-detectors as they reach the axis. The beam energy and magnetic field can be set such that the tritons from the (d, t) reaction are emitted at backwards lab angles and travel downstream while the protons from the (d, p) reaction travel upstream. The kinematics of particle motion inside solenoidal spectrometers is described in greater detail in Ref. [10] Additional detectors positioned downstream from the target to detect heavy ^{47,49}Ca recoils.

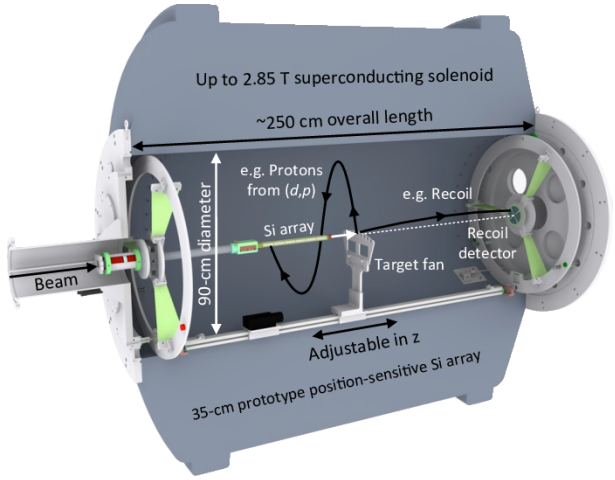

Figure 2. Annotated CAD rendering of HELIOS showing a typical set up for a (d, p) experiment as modified from Ref. [11].Whilst the schematic shows a typical (d, p) setup, the positioning of the recoil detector is also adjustable in z so as to enable accommodation of the downstream Si-array to detect the tritons.

For 15 years, the HELIOS device, as seen in Figure 2 (modified from Ref. [11]), has been equipped with a single Si array that has flexible positioning, upstream or downstream of the target. For the (d, p) reaction, protons are emitted upstream and there have been many successful works using this approach. However, with carefully chosen beam energies and the addition of a second Si array, it becomes kinematically feasible to simultaneously detect reaction products from different reactions that occur between the beam and target particles. For instance, by positioning a second Si-array downstream beyond the recoil detector, tritons from (d, t) reactions could be measured in parallel to protons from (d, p) reactions in the upstream array. In this work, we investigated this approach with beams of ^{48}Ca ions delivered to HELIOS. This is an important capability to demonstrate, particularly with regards to future programs that are planned with the SOLARIS device at FRIB.

2.1 Simultaneous $d(^{48}Ca,p)$ and $d(^{48}Ca,t)$ measurement: Attempt 1

In this experiment, a 10-MeV/u beam of ^{48}Ca ions delivered by the ATLAS superconducting linear accelerator was used to bombard deuterated (CD_2) targets of varying thicknesses in the range of 100-200 μg/cm^2. HELIOS was equipped with the standard 6×4 Si array positioned 800 mm downstream from the target position to detect tritons emitted from the (d, t) reaction, and a bespoke 2×4 Si array, built specifically for this test, positioned 50 mm upstream to detect protons from the (d, p) reaction. An additional recoil detector was positioned downstream, 750 mm from the target.

The downstream data collected during this measurement are represented in Fig. 3. Here, the energies of light ions that intercept the array are plotted as a function of distance along the solenoid axis. The six Si detector positions are clearly separated. Tritons from the (d, t) reaction travel downstream and were expected to be observed in this data set. However, the online data were dominated by light ions from other sources. Further inspection of the data offline, complemented by extensive modelling of every possible reaction that could take place, led to the discovery that the data were dominated by scattered protons and deuterons executing multiple orbits before being intercepted on-axis by the Si-detectors. This posed an additional issue, as a proton executing three orbits will have the same orbital time period as a triton. Nonetheless, faint signatures of tritons were visible (indicated by the red box at the centre of Fig. 3). The experiment was subsequently rescheduled and the HELIOS set up was modified to overcome the issues caused by scattering events from other reactions.

2.2 Simultaneous $d(^{48}Ca,p)$ and $d(^{48}Ca,t)$ measurement: Attempt 2

The HELIOS set up was modified for the second experiment. A long plastic pipe ~50 mm in length was positioned between the target and the downstream Si array,

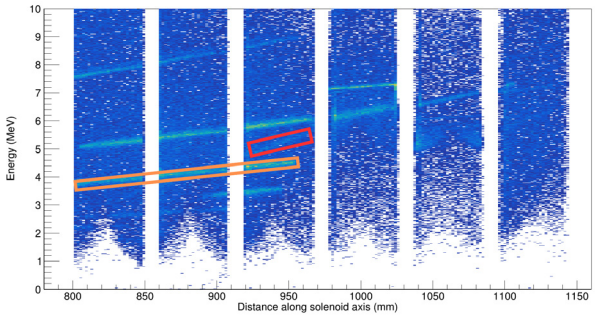

Figure 3. Data collected in the downstream array showing the energy of the detected particles plotted as a function of distance along solenoid axis, z. The strong kinematic lines all correspond to multi-orbit scattered protons and deuterons. For instance, the orange box encloses scattered deuterons undertaking two orbits. These events end up washing out the desired triton events which are faintly seen enclosed within the red box

which was moved further downstream to 900 mm to accommodate the blocker. The aim here was to block the path of protons and deuterons emitted from the target that would undergo multiple orbits before detection. Single-orbit trajectories would still be detected; however, software gating on the particle cyclotron period would allow unambiguous selection of tritons in the data. The effects of this adjustment are evident, with the tritons clearly elucidated in the spectrum shown in Fig. 4. The excitation-energy spectra constructed from the measured triton and proton transfer-reaction products of interest reveal excited states in ^{47,49}Ca, respectively. These are shown in Fig. 5. Results of the full analysis and their interpretation from this experiment are expected to form the subject of a separate publication; however, we note that this is the first-ever unambiguous demonstration of dual reaction studies with HELIOS using both the upstream and downstream directions. Similar experiments are expected to take place soon with the SOLARIS device at FRIB.

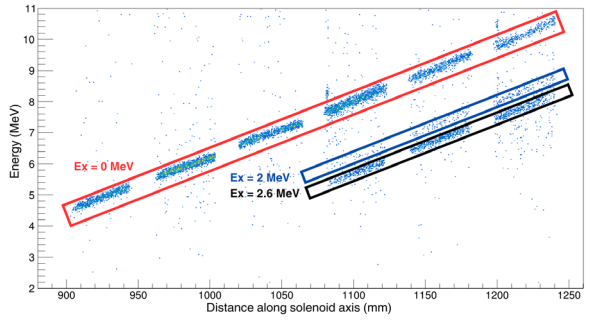

Figure 4. Data collected in the downstream array showing the energy of the detected particles plotted as a function of distance along solenoid axis, z after the addition of the blocker. This reveals a clean triton spectrum with the first three states of ^{47}Ca visible.

3 The Light-Ion (L-ion) Focal Plane Detector

Transfer reactions in inverse kinematics with solenoidal spectrometers are primarily intended to enable studies of radioactive isotopes. However, high-resolution particle spectroscopy can be achieved in regular kinematics with stable targets and light beams. This is particularly relevant for the investigation across the $N = 28$ chain beyond ^{48}Ca where systematic studies are necessary to firmly establish the evolution of structure in the region. As seen in Fig. 1: ^{50}Ti, ^{51}V, ^{52}Cr are all stable isotopes along the $N = 28$ chain. Thus, there is a need for devices to perform high-resolution particle spectroscopy in regular kinematics on the stable isotopes along the $N = 28$ chain.

To that end, the Enge Magnetic Spectrometer [15] at the Australian Heavy Ion Accelerator Facility (HIAF) has been equipped with a newly developed focal-plane detector to perform nucleon-transfer-reaction measurements with stable beams and targets. A partial CAD model of the Light-ion (L-ion) detector is shown in Fig. 6. The cathode (blue) and anode segments (orange) are separated by a Frisch grid. Position wires (red) are held in gridded channels at voltages around 2 kV. The position along the detector is inferred by measuring the time difference between the signals, caused by the avalanche localisation, at both ends of the wire. The energy loss as the particle travels through the detector volume is measured with two ΔE segments (brown) between the two position wires. A plastic scintillator bar (yellow) is positioned at the end of the detector volume and provides the stopped energy component of the particle signal. Particle identification is achieved through $\Delta E - E$ measurements, with the E measurements coming from either the cathode or the scintillator, and different stopping powers of the different light-ion species. Early experiments with the new system have primarily focused on the $N = 28$ isotones highlighted in Fig. 1.

The design and working principle of the detector is largely based on an older iteration, as described in Ref. [16]. However, a key difference with the new detector is the inclusion of the backing scintillator at the end of the detector volume. This is an important aspect of the design of L-ion as a device for single-nucleon transfer reactions, whereas the previous detector was predominantly used for heavier ions and multi-nucleon reactions. Bespoke software has been developed to use the new detector with an XIA Pixie16 digital data acquisition system.

The effectiveness of this setup for high-resolution particle spectroscopy was demonstrated in recent in-beam tests with states of ^{53}Cr visible from the ^{52}Cr$(d, p)^{53}$Cr reaction (E_d = 12 MeV). A sample time-difference spectrum along the front position wire is shown in Fig. 7. Measurements were also taken on titanium and iron isotopes. Analysis of the data on (d, p) reactions on ^{54}Fe, ^{52}Cr, and ^{50}Ti are presently underway with a focus on obtaining the spectroscopic strengths of the first $f_{\frac{7}{2}}$ and $p_{\frac{3}{2}}$ states. This is in addition to serving as a proof-of-principle for the detector and benchmarking its constituent components. Further experiments are planned, both with the same $N = 28$ isotones and also with odd-Z isotones like ^{51}V. The L-

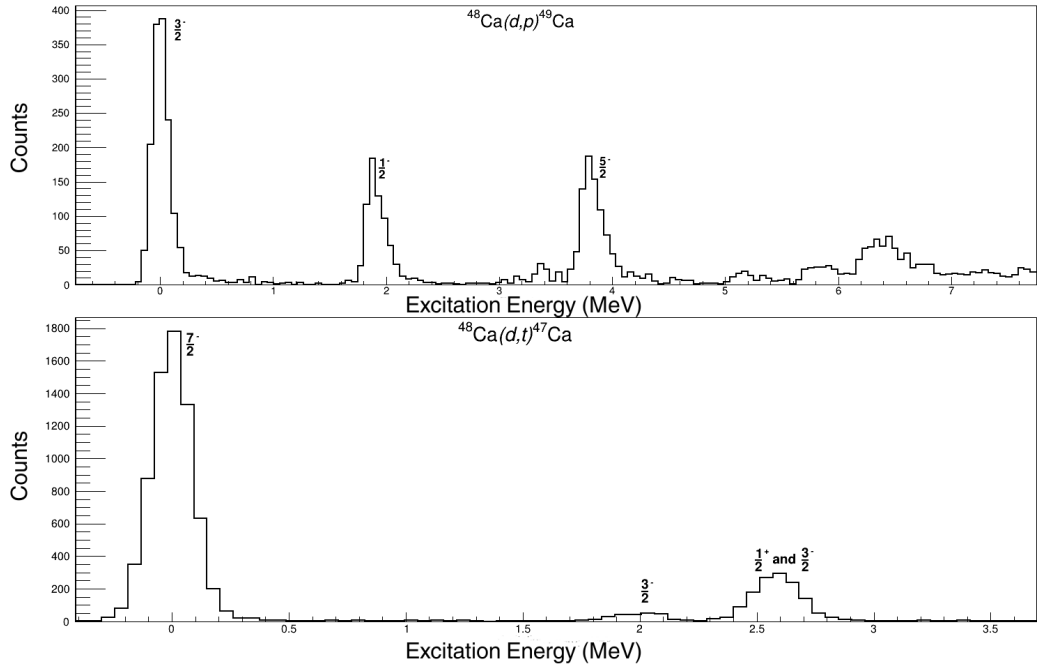

Figure 5. Excitation-energy spectra measured for the (d, p) and (d, t) reactions respectively with tentative assignments for selected states populated in $^{49,\ 47}$Ca

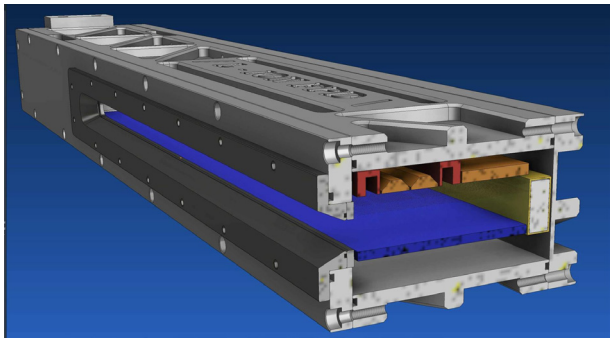

Figure 6. CAD model of the Light-ion Focal Plane Detector. See text for details.

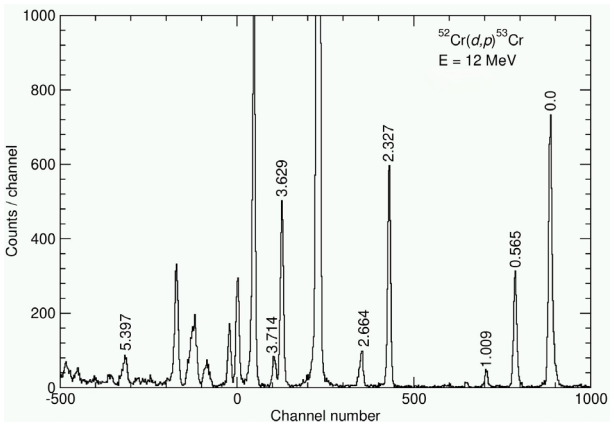

Figure 7. Position-wire spectrum with selected states of ^{53}Cr identified. The peaks that go off scale are from target contaminants, typically oxygen and carbon. The uncalibrated spectrum suffices to demonstrate the identification of states of ^{53}Cr while a proper calibration requires careful consideration of edge-effects in the detector and incorporation of non-linearties in time-difference responses at the ends of the detector.

ion detector will also leverage expected future capabilities at HIAF and enable transfer reaction studies with $^{3,\ 4}$He beams.

4 Conclusions and future work

We report on the first ever simultaneous (d, p) and (d, t) reaction study performed in inverse kinematics with the HELIOS solenoidal spectrometer at Argonne National Laboratory. This demonstration will hopefully pave the way for future experiments of similar design, particularly with the SOLARIS device at FRIB. Consistent, systematic investigation with single-nucleon transfer reactions is necessary to elucidate the nature of strength fragmentation in the $N = 28$ region. Such studies may also have ancillary benefits for neutrinoless double-beta decay searches, and aid future investigations into the emerging $N = 32$, 34 shell closures in this region. The new L-ion detector, with the Enge Magnetic Spectromter at HIAF, enables complementary studies with stable targets and light beams to be performed. This has the advantage of enabling high-resolution particle spectroscopy at a wider range of measurement angles than can currently be achieved with reactions performed in inverse kinematics experiments with solenoidal spectrometers.

Acknowledgements

This work is supported by the Australian Research Council Grant No. DP210101201, the International Technology Center Pacific (ITC-PAC) u nder C ontract No. FA520919PA138, the Australian National University Major Equipment Committee, the US Department of Energy, Office of Nuclear Physics, under Contract No . DE-AC02-06CH11357, and the U. S. Department of Energy, Grant No. DE-SC0014552. The authors would like to acknowledge the ATLAS operations team for successful beam delivery. This research used resources of ANL's ATLAS facility, which is a DOE Office of Science User Facility.

References

[1] A. E. Stuchbery and J. L. Wood, To Shell Model, or Not to Shell Model, That Is the Question, Physics **4**, 697 (2022). https://doi.org/10.3390/physics4030048

[2] H. L. Crawford *et. al.*, Unexpected distribution of $\nu 1f_{7/2}$ strength in ^{49}Ca, Phys. Rev. C **96**, 064317 (2017). https://doi.org/10.1103/PhysRevC.95.064317

[3] Y. Uozumi *et. al.*, Single-particle strengths measured with ^{48}Ca$(d,p)^{49}$Ca reaction at 56 MeV, Nucl. Phys. A **576**, 123 (1994). https://doi.org/10.1016/0375-9474(94)90740-4

[4] M. E. Williams-Norton and R. Abegg, Study of low-lying levels in 47Ca with the ^{48}Ca$(d,t)^{47}$Ca reaction, Nucl. Phys. A **291**, 429 (1977). https://doi.org/10.1016/0375-9474(77)90330-X

[5] M. Horoi *et al.*, Statistical analysis for the neutrinoless double-β-decay matrix element of ^{48}Ca, Phys. Rev. C **106**, 054302 (2022). https://doi.org/10.1103/PhysRevC.106.054302

[6] F. Weinholtz *et. al.*, Masses of exotic calcium isotopes pin down nuclear forces, Nature **498**, 346 (2013). https://doi.org/10.1038/nature12226

[7] A. Koszorus *et. al.*, Charge radii of exotic potassium isotopes challenge nuclear theory and the magic character of $N = 32$, Nature **17**, 439 (2021). https://doi.org/10.1038/s41567-020-01136-5

[8] D. Steppenbeck *et. al.*, Evidence for a new nuclear 'magic number' from the level structure of ^{54}Ca, Nature **502**, 207 (2013). https://doi.org/10.1038/nature12522

[9] S. Chen *et. al.*, Quasifree Neutron Knockout from ^{54}Ca Corroborates Arising $N = 34$ Neutron Magic Number, Phys. Rev. Lett. **123**, 142501 (2019). https://doi.org/10.1103/PhysRevLett.123.142501

[10] A. H. Wuosmaa *et al.*, A solenoidal spectrometer for reactions in inverse kinematics, Nucl. Instrum. Methods Phys. Res., Sect. A **580**, 1290 (2007). https://doi.org/10.1016/j.nima.2007.07.029

[11] J. C. Lighthall *et. al.*, Commissioning of the HELIOS spectrometer, Nucl. Instrum. Methods Phys. Res., Sect. A **622**, 97 (2010). https://doi.org/10.1016/j.nima.2010.06.220

[12] J. Chen *et. al.*, Evolution of the nuclear spin-orbit splitting explored via the ^{32}Si$(d,p)^{33}$Si reaction using SOLARIS, Phys. Lett. B **853**, 138679 (2024). https://doi.org/10.1016/j.physletb.2024.138678

[13] N. Watwood *et. al.*, Valence $1s-0d$ proton vacancy of the ^{32}Si ground state, Phys. Rev. C **112**, 054304 (2025). https://doi.org/10.1103/4lzs-mv3l

[14] T. L. Tang *et. al.*, First Exploration of Neutron Shell Structure below Lead and beyond $N = 126$, Phys.Rev. Lett. **124**, 062502 (2020). https://doi.org/10.1103/PhysRevLett.124.062502

[15] J. E. Spencer and H. A. Enge, Split-pole magnetic spectrograph for precision nuclear spectroscopy, Nucl. Instrum. Methods **49**, 181 (1967). https://doi.org/10.1016/0029-554X(67)90684-2

[16] T. R. Ophel and A. Johnston, A focal plane detector for both light and heavy ions, Nucl. Instrum. Methods **157**, 461 (1978). https://doi.org/10.1016/0029-554X(78)90005-8